Heavy Atom Effect on the Charge Recombination Dynamics of Photogenerated Geminate Ion Pairs

Olivier Nicolet and Eric Vauthey*

Department of Physical Chemistry, University of Geneva, 30 quai Ernest Ansermet, CH-1211 Geneva 4, Switzerland

Received: December 5, 2002; In Final Form: April 23, 2003

The charge recombination dynamics of geminate ion pairs formed by electron transfer quenching of cyanoanthracene derivatives by bromo- and iodo-anisole in acetonitrile was investigated using various ultrafast spectroscopic techniques. Without a heavy atom, the only charge recombination pathway is that leading to the neutral ground state. With heavy atom substituted anisoles, charge recombination to the local triplet state of the excited precursor is observed. Time constants for triplet charge recombination ranging from 400 ps to less than 10 ps, depending on the heavy atom and on the energy gap between the ion pair and the triplet state, have been measured. This heavy atom effect was observed with ion pairs formed upon electron-transfer quenching with driving force going from −0.15 to −0.6 eV, suggesting that these intermediates are in fact exciplexes. A new scheme for producing free ions with a high yield using this effect and a secondary electron donor is also demonstrated.

Introduction

Over the past decades, the charge recombination (CR)[1] dynamics of geminate ion pairs (GIP) produced by photoinduced bimolecular electron transfer has been intensively investigated.[2−14] For many applications, the occurrence of this energy wasting process following charge separation (CS) has to be minimized and it is therefore of paramount importance to know how to influence its dynamics. Among the many factors, which have been shown to affect the CR dynamics of GIPs, the driving force, ΔG_{CR}, and the spin multiplicity are probably the most important. Indeed, the free energy dependence of the CR rate constant, k_{CR}, is in general discussed within the theory of nonadiabatic electron-transfer reaction.[15,16] In general, CR is in the inverted regime, and therefore, k_{CR} decreases with increasing the energy gap between the GIP, ($M^{+/-}Q^{-/+}$), and the neutral ground state, M + Q, where M is the reactant undergoing photoexcitation and Q is the quencher. For example, k_{CR} has been shown to vary by more than 3 orders of magnitude by changing ΔG_{CR} from about −1 to −3 eV.[3,13] If spin-forbidden, geminate CR can be totally suppressed in a polar and nonviscous solvent like acetonitrile. If the excited precursor is in the triplet state, the ensuing GIP is formed in the triplet state as well and CR to the neutral ground state is spin forbidden. If this GIP can dissociate into free ions in a time scale much shorter than that of hyperfine coupling, the efficiency of geminate CR is essentially zero. This is the case for example with the system benzophenone/1,4-diazabicyclo[2,2,2]octane (DABCO) in acetonitrile for which a free ion yield of unity has been reported.[17,18]

However, the formation of a triplet GIP does not warrant a high free ion yield. For example, the free ion yield measured upon CS between xanthone in the triplet state (^{3}M*) and 1-methoxynaphthalene (Q) in ACN amounts to 0.12 only.[19] This relatively low yield is due to the presence of the M + ^{3}Q* state below the GIP state. In this case, CR of the triplet GIP to this neutral excited state is not spin-forbidden and competes efficiently with dissociation to free ions.[19]

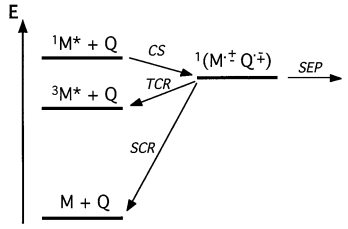

Figure 1. Energy diagram of the states involved in the charge separation between an excited precursor (M*) and a quencher (Q).

Many excited precursor, M*, have a relatively large S_1-T_1 energy gap, and if CS is weakly to moderately exergonic, the ensuing GIP may lies above the ^{3}M* + Q state as shown in Figure 1. Although energetically favorable, this triplet charge recombination (TCR) is spin forbidden. Nevertheless, this process can be operative under certain circumstances:[20,21]

(1) TCR can take place after a spin-flip to the triplet GIP induced by the hyperfine interaction. For GIPs composed of typical aromatic hydrocarbons, this process occurs in the 10−100 ns time scale. For example, Weller and co-workers have reported a rate constant of singlet−triplet conversion of 6×10^7 s^{-1} for a GIP composed of pyrene anion and dimethylaniline cation in methanol.[22] In a solvent like acetonitrile, this is substantially slower than the dissociation of the GIP, and therefore, TCR is negligible. This mechanism requires the singlet and triplet GIP states to be nearly degenerate; that is, the exchange interaction in the GIP has to be very weak.[23] This implies that the ions have a negligibly small orbital overlap. Such a GIP corresponds to what is usually called a solvent separated ion pair (SSIP) or a loose ion pair (LIP). The influence of the orbital overlap on the hyperfine interaction has been very clearly demonstrated by Roest et al. in an investigation of the distance dependence of TCR in a series of covalently linked donor−acceptor systems.[24] TCR via hyperfine interaction can

* To whom correspondence should be addressed. E-mail: eric.vauthey@chiphy.unige.ch.

10.1021/jp0276247 CCC: $25.00
Published on Web 07/11/2003

be substantially slowed by the presence of an external magnetic field, which lifts the degeneracy of the triplet sublevels and reduces the transition probability between the singlet and the $T_{\pm 1}$ states.[25]

(2) CS may also result to an ion pair with substantial orbital overlap. Such a GIP is designed as a contact ion pair (CIP) or as an exciplex. In principle, a CIP is the limiting case of an exciplex with a full charge transfer. However, if the ions are truly in close contact, some orbital overlap cannot be avoided, and therefore, a full charge transfer is hardly possible, especially with ions characterized by strongly delocalized orbitals. In this case, TCR to $^3M^* + Q$ can be viewed as an intersystem crossing. As spin−orbit coupling (SOC) is in general weak in aromatic hydrocarbons, this pathway is not a dominant decay mechanism of the exciplex in polar solvents. For example, Weller and co-workers have reported TCR time constants of the order of 100 ns for the pyrene/dimethylaniline exciplex in solvents of various polarity.[22] Nevertheless, Okada et al. have reported a TCR time constant as short as 40 ps in an intramolecular exciplex in hexane.[26] This fast TCR was ascribed to a large SOC because of the nature of the orbitals involved in the charge transfer as well as to the large orbital overlap of the donor and acceptor moieties. This overlap is much smaller in polar solvents and therefore the TCR time constant of the same molecule in acetonitrile was considerably larger, around 1.5 ns.[26] SOC can be strongly enhanced by the presence of heavy atoms on the reactants. The heavy atom effect has therefore been used as a mechanistic tool to prove the involvement of exciplexes in photoinduced ET processes. For example, Steiner and Winter have reported a strong reduction of the free radical yield in the ET quenching of thionine in the triplet state upon heavy atom substitution of the quencher.[27] This was explained by a heavy atom enhanced deactivation of the triplet exciplex, the quenching product, to the neutral singlet ground state, competing with its dissociation to free radicals. More recently, Steiner and co-workers have reported a similar heavy atom effect but for an exciplex formed by ET quenching of a precursor in the singlet state.[28] In this case, the decrease of the free radical yield was due to the enhanced TCR of the singlet exciplex.

Similarly, Kikuchi and co-workers have observed a heavy atom induced decrease of the free ion yield in the quenching of 9,10-dicyanoanthracene in the S_1 state by a series of halogenated anisoles in acetonitrile.[29] However, no effect was observed when using halogenated anilines as electron donors. This difference was explained by an effect of the driving force of ET quenching, ΔG_{CS}, on the nature of the primary product. ET quenching with anisoles is weakly exergonic, $\Delta G_{CS} > -0.3$ eV, and thus results to an exciplex, whose lifetime depends on heavy atom substitution. On the other hand, CS with anilines, is more exergonic, $\Delta G_{CS} < -1.0$ eV, and directly results to a LIP, which can only undergo TCR through the less efficient hyperfine interaction.[29]

The above-mentioned investigations have been performed by monitoring the CS product in the microsecond time scale using laser flash photolysis. Although very useful to obtain triplet and free ion yields, this time scale is much too large to have directly access to the primary quenching product, i.e., the geminate ion pair (CIP or LIP), which decays in less than a few nanosecond in acetonitrile.[30] Moreover, the triplet state can also be populated upon homogeneous recombination of the free ions. Because of spin statistics, 3/4 of the ion encounters result to a triplet geminate ion pair, for which TCR is spin allowed. Therefore, when measuring in the microsecond time scale, the distinction between the triplet population formed upon geminate CR and that formed upon homogeneous CR may be problematic.[31]

We present here, what is to our knowledge, the first direct measurements of the heavy atom effect on the CR dynamics of GIPs in acetonitrile. The GIPs are formed upon CS between photoexcited cyanoanthracene derivatives and halogenated anisoles. The dynamics of singlet excited state, ion pair, and triplet state populations were measured using the fluorescence up-conversion and the multiplex transient grating (TG) techniques. The latter method gives essentially the same information as transient absorption but has a superior sensitivity.[32]

We will also demonstrate that the heavy atom effect can be used efficiently to produce free ions in a high yield with an excited precursor in the singlet state and independently of ΔG_{CR}.

Experimental Section

Measurements. Two different TG setups, depending on the time scale of the measurement, have been used. The ps TG setup, which has been described in detail in ref 32, was used for measurements between 30 ps and 2 ns. Excitation was performed with two time coincident pulses at 355 nm generated by frequency tripling the output of an active/passive mode-locked Q-switched Nd:YAG laser (Continuum PY-61-10). The duration of the pulses was about 25 ps and the total pump intensity on the sample was around 5 mJ/cm^2.

The fs TG setup, which has been described in detail in ref 13, was used for measuring processes occurring in a time scale shorter than about 50 ps. Excitation was performed using the frequency doubled output of a standard 1 kHz amplified Ti: sapphire system (Spectra-Physics). The duration of the pulses at 400 nm was around 100 fs. All TG spectra were corrected for the chirp of the probe pulse.

The fluorescence up-conversion setup has already been described in ref 33. Excitation was achieved at 400 nm, using the frequency-doubled output of a Kerr lens mode-locked Ti: sapphire laser (Tsunami, Spectra-Physics).

The free ion yield has been determined using photoconductivity.[34] The photocurrent cell has been described in detail previously.[35] The samples were excited at 355 nm using the output of the ps Nd:YAG laser. The system benzophenone with 0.02 M 1,4-diazabicyclo[2,2,2]octane in acetonitrile, which has a free ion yield of unity, was used as a standard.[36]

Samples. 9,10-Dicyanoanthracene (DCA, Kodak) was recrystallized. 2,9,10-Tricyanoanthracene (TrCA) and 2,6,9,10-tetracyanoanthracene (TeCA) were synthesized according to the litterature.[37] Anisole (ANI), 2-bromoanisole (BrANI, Acros), 2-iodoanisole (IANI), and *N*,*N*-dimethylaniline (DMA) were vacuum distilled. Acetonitrile (ACN, UV grade) was used as received. Unless specified, all chemicals were from Fluka.

For TG measurements, the sample solutions were placed in a quartz cell of 1 mm path-length, and their absorbance at 355 or 400 nm was around 0.2. During the experiments, the sample solutions were continuously stirred by N_2 bubbling. For fluorescence up-conversion, a rotating cell with an optical path-length of 0.4 mm was used. The absorbance of the samples at 400 nm was around 0.1. No significant sample degradation was observed after the measurements.

Results

DCA + Donors. Figure 2A shows the transient grating (TG) spectra measured with DCA and 1 M ANI, at different time delays after excitation at 355 nm. As explained in detail elsewhere, a TG spectrum is very similar to a transient absorption spectrum, the major difference being that the TG intensity is always positive.[32] This is due to the fact that the TG signal intensity is proportional to the square of the

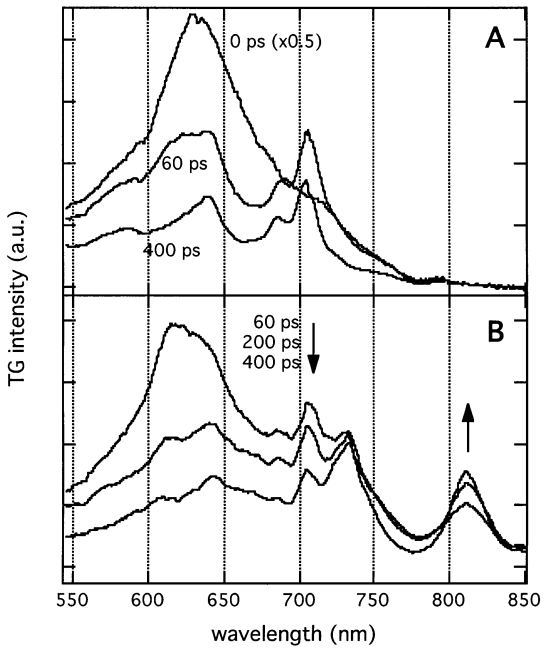

Figure 2. TG spectra measured at various time delays after excitation at 355 nm of solutions of (A) DCA + 1 M ANI and (B) DCA + 1 M BrANI in ACN.

concentration changes.[38,39] The strong TG band measured at short time delay and centered at 620 nm is due to a $S_1 \rightarrow S_n$ transition of DCA*.[40] As the time delay is increased, this band vanishes and is replaced by a spectrum with bands at 705, 685, 640, and 583 nm, which is due to $DCA^{\bullet -}$, as already reported in ref 30. The radical cation of ANI, which absorbs weakly at 445 nm,[41] is not visible in the spectral window used for these measurements.

The time dependence of the square root of the TG intensity at 705 nm, which reflects the $DCA^{\bullet -}$ concentration, exhibits an exponential decay, with a time constant of 290 ps, to a constant value different from zero. The small residual intensity is due to the free ion population, which decays in the microsecond time scale by homogeneous recombination. The 290 ps component corresponds to the decay of the $DCA^{\bullet -}/ANI^{\bullet +}$ GIP population, by both singlet CR to the neutral ground state (SCR) and separation into free ions. As already discussed in ref 30, the rate constants of SCR and dissociation, k_{SCR} and k_{sep}, can be determined from the rate constant of ion population decay, k_{pop}, and the free ion yield, Φ_{ion}

$$\Phi_{ion} = \Phi_q \Phi_{sep} = \Phi_q \frac{k_{sep}}{k_{pop}} = \Phi_q \frac{k_{sep}}{k_{sep} + k_{SCR}} \qquad (1)$$

where Φ_q and Φ_{sep} are the quenching efficiency and the separation efficiency, respectively. For the system DCA/ANI in ACN, Φ_{sep} amounts to 0.13,[30] and thus, k_{SCR} and k_{sep} are equal to 3 and 0.45 ns^{-1}, respectively, in agreement with previous measurements.[30]

Figure 2B shows the TG spectra measured with DCA and 1 M BrANI in ACN at different time delays after excitation. Near zero time delay, the TG spectrum is essentially the same as that measured with ANI. After about 70 ps, the 705, 685, and 640 nm bands of $DCA^{\bullet -}$ appear, but two new bands at 735 and 811 nm can be observed as well. As the time delay increases further, the $DCA^{\bullet -}$ bands become relatively smaller than the 735 nm band, while the intensity of the 811 nm band increases markedly. After about 700 ps, the TG spectra remains unchanged and consists of bands at 811, 735, and 705 nm as well as of a broad band extending from 550 to 700 nm with small maxima at 685 and 640 nm. The 705 nm band and the broad band are due to free $DCA^{\bullet -}$, whereas the new features at 811 and 735 nm can be assigned to ^{3}DCA*. This is confirmed by measurements of Kikuchi and co-workers who have observed a band at 805 nm in the transient absorption spectrum measured 20 μs after excitation of the system DCA/4-bromoanisole in ACN.[29] However, the spectral resolution of their measurement did not allow the 735 nm band of ^{3}DCA* to be distinguished from the 705 nm band of $DCA^{\bullet -}$.

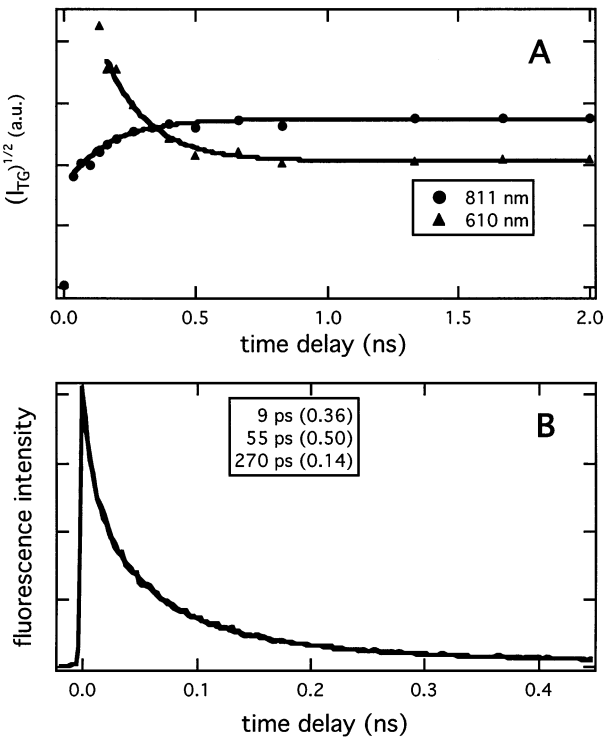

Figure 3. (A) Time profiles of the square root of the TG intensity measured with DCA + 1 M BrANI in ACN. The profile at 610 nm reflects $DCA^{\bullet -}$ population and that at 811 nm the ^{3}DCA* population. (B) Time evolution of the ^{1}DCA* fluorescence intensity at 465 nm in the presence of 1 M BrANI in ACN and best fit (the time constants and the associated amplitudes are given in the inset).

Figure 3A shows the time profiles of the square root of the TG intensity at 610 and 811 nm. As it can be seen in Figure 2B, apart from the 811 nm ^{3}DCA* band, the spectra of ^{1}DCA*, $DCA^{\bullet -}$, and ^{3}DCA* strongly overlap, and the determination of the dynamics of ^{1}DCA* and $DCA^{\bullet -}$ populations is difficult. Therefore, the time evolution of the ^{1}DCA* population has been measured selectively by fluorescence up-conversion. As illustrated by Figure 3B, the fluorescence decay of ^{1}DCA* with 1 M Br-ANI in ACN is not monoexponential but can be reproduced using the sum of three exponential functions with the parameters shown in the inset. This nonexponential decay is due to the so-called transient effect, which is particularly strong at high quencher concentrations.[42] According to this figure, the contribution of the ^{1}DCA* population to the TG intensity after a time delay of about 200 ps can be considered as negligible. The decay of the TG intensity at 610 nm, due essentially to $DCA^{\bullet -}$ population, can be fitted using an exponential function with a time constant of 170 ps. The same value is obtained by exponential fit of the time profile at 811 nm. This is a clear indication that ^{3}DCA* is generated from the $DCA^{\bullet -}/BrANI^{\bullet +}$ GIP.

With BrANI, the rate constant of the decay of the ion pair population is $k_{pop}(BrANI) = k_{SCR} + k_{TCR} + k_{sep}$. As the

oxidation potentials of ANI and BrANI are almost identical (E_{ox}(ANI) = 1.76 V vs SCE, E_{ox}(BrANI) = 1.80 V vs SCE),[28] the driving force of SCR is independent of heavy atom substitution. We will assume that the perturbation due to the bromine atom is not strong enough to substantially affect k_{SCR}. In other words, we will assume that k_{SCR}(BrANI) = k_{SCR}(ANI). In this case, the rate constant for TCR, k_{TCR}, can be calculated as $k_{TCR} = k_{pop}(\text{BrANI}) - k_{pop}(\text{ANI}) = 2.43\ \text{ns}^{-1}$. As $k_{sep} \ll k_{pop}$, the assumption that k_{sep} is the same for both GIPs should not introduce a significant error on k_{TCR}. With this value and k_{pop}(BrANI), the triplet yield can now be calculated as $\Phi_T = k_{TCR}/k_{pop}(\text{BrANI}) = 0.41$. This triplet yield is in good agreement with the Φ_T value of 0.49 reported by Kikuchi and co-workers with DCA/4-bromoanisole.[29] However, the results obtained here with BrANI (2-bromoanisole) and those with 4-bromoanisole should be compared with caution, because the heavy atom effect on ET has been reported to depend markedly on the relative position of the halogen atom on the benzene ring.[27]

The same TG measurements have been repeated with 1 M IANI in ACN. At early time, the TG spectrum is dominated by the ^{1}DCA* band. As this band decays, the 811 and 735 nm ^{3}DCA* bands appear. No spectral feature that could be assigned to DCA$^{\bullet-}$ can be observed. The rise time of the ^{3}DCA* population determined from the TG intensity at 811 nm amounts to 60 ps and is, within the experimental error, equal to the decay time of the ^{1}DCA* population. The TG spectrum measured after 500 ps, which should be due to ^{3}DCA* only, is shown in Figure 4A. One can see that, in addition to the 811 and 735 nm bands, ^{3}DCA* has a band at 675 nm. This band cannot be distinguished if DCA$^{\bullet-}$ is also present. By comparing the intensity of the 811 nm TG band with BrANI and IANI, a triplet yield of 0.95 ± 0.05 is obtained for DCA/IANI.

To detect the presence of DCA$^{\bullet-}$, the measurements were also performed using 2 M IANI and with the fs TG setup. The spectrum above 760 nm cannot be observed with this setup because of the instability of the white light continuum in this spectral region. As shown in Figure 4B, a small peak around 705 nm can be seen at time delays around 40 ps. This peak has almost totally vanished at 100 ps. The time profile of the square root of the TG intensity at 600 and 705 nm could be reasonably will fitted by a single-exponential function with lifetimes of 26 and 35 ps, respectively. The decay of the ^{1}DCA* fluorescence measured by up-conversion with 2 M IANI could be reproduced by a biexponential function with time constants of 3.4 and 25 ps. The 26 ps decay obtained above can thus be assigned to the ^{1}DCA* population, the time increment used in the TG experiment being too large (∼4 ps) to resolve the 3.4 ps component.

The determination of the rate constant of TCR from these data is not straightforward as ^{1}DCA*, DCA$^{\bullet-}$, and ^{3}DCA* population contribute to the 705 nm TG intensity. To estimate k_{TCR}, the 705 nm TG intensity has been simulated using the information obtained from fluorescence up-conversion, by taking $k_{sep} = 0.45\ \text{ns}^{-1}$ and by varying the k_{TCR} and k_{SCR} values, while keeping $\Phi_T = 0.95$. To achieve this, the absorption coefficients of ^{1}DCA*, DCA$^{\bullet-}$, and ^{3}DCA* at 705 nm are needed. According to the literature, ϵ_{705}(DCA$^{\bullet-}$) = 8100 $\text{M}^{-1}\ \text{cm}^{-1}$.[29] A value of $\epsilon_{705}(^1\text{DCA*}) = 7000\ \text{M}^{-1}\text{cm}^{-1}$ was obtained by using the TG spectra measured with DCA + 0.3 M ANI. The TG spectrum at time zero is due to ^{1}DCA* only, whereas the TG spectrum at 1 ns is due to DCA$^{\bullet-}$. Knowing the time dependence of DCA$^{\bullet-}$, the 705 nm TG intensity was extrapolated to time zero and compared with that of ^{1}DCA*, assuming a quenching efficiency of unity. A similar procedure was used to determine the $\epsilon_{705}(^3\text{DCA*})$. In this case, the system DCA + 0.3 M BrANI was used and the TG spectra of ^{1}DCA* and ^{3}DCA where compared assuming a triplet yield of 0.41. This resulted in $\epsilon_{705}(^3\text{DCA*}) = 3400\ \text{M}^{-1}\ \text{cm}^{-1}$. Figure 4C shows the time profiles of the square root of the 705 nm TG intensity together with simulation obtained with k_{TCR} values ranging from 20 to 80 ns^{-1}. The best agreement with the experimental points is obtained with 30 $\text{ns}^{-1} < k_{TCR} < 50\ \text{ns}^{-1}$. Taking the average value $k_{TCR} = 40\ \text{ns}^{-1}$ gives $k_{SCR} = 1.6\ \text{ns}^{-1}$ and a separation efficiency Φ_{sep} of 0.01. The latter value is in good agreement with the TG measurements: no DCA$^{\bullet-}$ band can be observed after about 150 ps, indicating a very small free ion population. On the other hand, because of the rather large error on Φ_T, the value of k_{SCR} carries a too large uncertainty to be really meaningful.

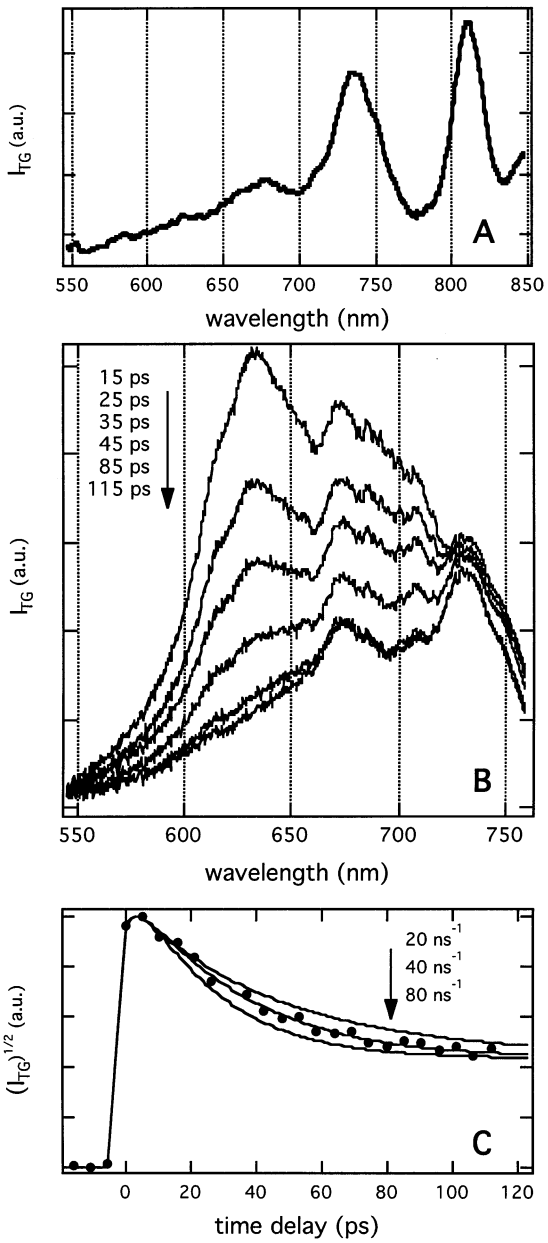

Figure 4. (A) TG spectrum measured 600 ps after excitation at 355 nm of a solution of DCA and 1 M IANI in ACN. (B) TG grating spectra measured at various time delays after excitation at 400 nm of a solution of DCA and 2 M IANI in ACN. (C) Time profile of the square root of the TG intensity at 705 nm measured with a solution of DCA and 2 M IANI in ACN (400 nm excitation). The continuous lines are simulations using various k_{TCR} values.

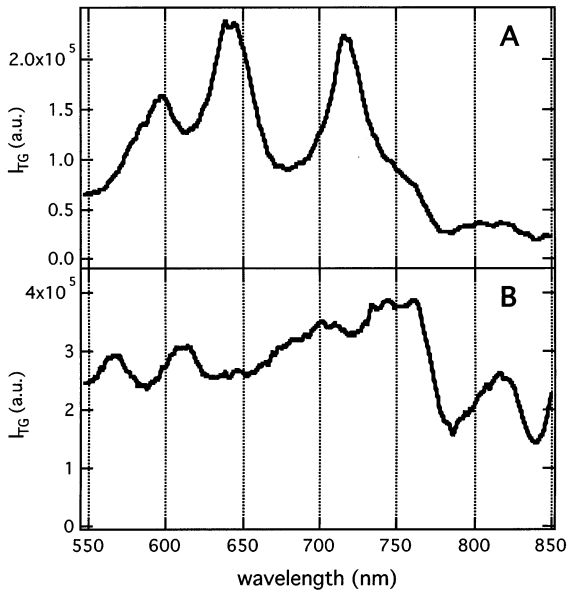

Figure 5. TG spectra measured (A) 170 ps after excitation at 355 nm of a solution of TrCA and 1 M ANI and (B) 300 ps after excitation of a solution of TrCA and 1 M IANI in ACN.

IANI with Stronger Electron Acceptors. To test the relationship between the driving force of CS, ΔG_{CS}, and the heavy atom effect on CR, the systems TrCA/IANI and TeCA/IANI were also investigated. Figure 5A shows the TG spectrum obtained 170 ps after excitation of a solution TrCA with 1 M ANI in ACN. At this time delay, the ^{1}TrCA* population, which exhibits a band with maximum at 649 nm, has totally decayed. The spectrum consists of three bands at 718, 643, and 593 nm. This agrees very well with the absorption spectrum of TrCA$^{\bullet-}$ prepared by γ irradiation in a methyl-tetrahydrofuran matrix at 77 K.[43] As already reported previously, the rate constant for the decay of ion population amounts to $k_{pop} = 15.8$ ns^{-1} and $\Phi_{sep} = 0.04$.[13] This results in k_{SCR} and k_{sep} values of 15.2 and 0.6 ns^{-1}, respectively.

Figure 5B, shows the TG spectrum of TrCA with 1 M IANI 300 ps after excitation. This spectrum, which is totally different from that of TrCA$^{\bullet-}$, remains constant on longer time delays and is ascribed to ^{3}TrCA* generated by TCR. The formation of ^{3}TrCA* is so fast that, with the time resolution of the ps TG setup and 1 M IANI, the formation of TrCA$^{\bullet-}$ can only be guessed as a small shoulder around 720 nm during the decay of the ^{1}DCA* band. Consequently, the measurements were also performed with the fs TG setup using with higher IANI concentration. However, even at a 2 M IANI, the decay of the ion TG band occurs in the same time scale that of the singlet precursor. A decay time of 9.5 ps, which can be considered as an upper limit of the ion population lifetime, was obtained.

Similar measurements were performed with the stronger acceptor, TeCA. The ion pair dynamics of TeCA/ANI has been investigated in detail elsewhere.[13] SCR occurs with a rate constant of $k_{SCR} = 47.6$ ns^{-1}. This process is much faster than separation of the GIP to the free ions, and therefore, no significant free ion population could be detected. The TG spectrum of the TeCA$^{\bullet-}$ exhibits bands at 600, 656, and 725 nm.

At short time delay ($\leq$15 ps), the TG spectrum measured with TeCA and 1.5 M IANI exhibits a broad band centered around 650 nm and dominated by ^{1}TeCA*. Weak features, that could be associated with TeCA$^{\bullet-}$, can be observed at 600 and 725 nm, and a band at 765 nm is also present. This spectrum

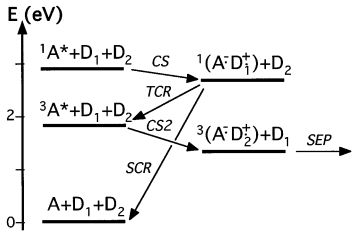

Figure 6. Energy diagram of the states involved in the ternary systems A + IANI + DMA (D_1, IANI; D_2, DMA). For the sake of clarity, only the most important processes are included.

evolves to another of smaller intensity with maxima at 600, 650−690, and 765 nm, which remained unchanged as the time delay is increased and which is assigned to ^{3}TeCA*. In this case again, the decay of the TeCA$^{\bullet-}$ occurs within the lifetime of ^{1}TeCA* and only an upper limit decay time of 7 ps can be determined.

Reactions with a Secondary Electron Donor. To test whether the species observed with the systems TrCA/IANI and TeCA/IANI are really ^{3}TrCA* and ^{3}TeCA* and in order to estimate Φ_T, measurements with a secondary electron donor were performed. This secondary donor has to be strong enough to quench the acceptor in the triplet state. If such a quenching occurs, the resulting GIP is in the triplet state, and CR to the singlet ground state is spin forbidden. Therefore, this triplet GIP should predominantly decay by separation into free ions, and the free ion yield should reflect the triplet yield. The secondary donor was DMA and the main processes occurring in these ternary systems are shown in Figure 6. The triplet state energy is only known for DCA, for which values of 1.66[29] and 1.81 eV[44] have been reported. As the triplet state energy of most anthracene derivatives lies between 1.66 and 1.85 eV,[44] it is reasonable to assume that those of TrCA and TeCA are in this range as well.

Figure 7A shows the TG spectra measured at different time delays after excitation at 355 nm of a solution of TrCA with 1 M IANI and 0.075 M DMA in ACN. During the first 100 ps, the TG spectra are similar to those measured with TrCA/IANI. However, at longer time delay, TG bands at 718, 643, and 593 nm and due to TrCA$^{\bullet-}$ grow. After about 2 ns, the TG spectrum is due to TrCA$^{\bullet-}$ only. As DMA$^{\bullet+}$ absorbs only weakly below 500 nm,[41] its contribution to the TG spectra cannot be seen. The same behavior has been observed with TeCA + 1M IANI and 0.075 M DMA in ACN as shown in Figure 7B. Figure 7C shows the time profile of the square root of the TG intensity at 600 nm. This profile can be well reproduced by a biexponential function, with a rise time of the TeCA$^{\bullet-}$ population of 670 ps. This value and the DMA concentration of 0.075 M give a second-order rate constant of ^{3}TeCA* quenching of 2×10^{10} M^{-1} s^{-1}, indicating a diffusion controlled process.

Figure 6 shows that the quenching of the singlet precursor by DMA is also possible. This process results in a GIP in the singlet state, for which SCR is not spin forbidden. Moreover, as the driving force for CR of these GIPs is no longer highly exergonic, CR is not in the inverted but rather in the barrierless regime and is thus ultrafast. Indeed, we have recently reported k_{SCR} values of 500 and 870 ns^{-1} for TrCA$^{\bullet-}$/DMA$^{\bullet+}$ and TeCA$^{\bullet-}$/DMA$^{\bullet+}$, respectively.[13] Consequently, this singlet quenching process does not lead to a free ion population. As this population is only due to the triplet quenching process, the free ion yield is an indirect measure of the triplet yield. The free ion yield was measured using photoconductivity. For these measurements, the concentration of anisole was 0.1 M. This concentration is large enough to ensure an efficient quenching

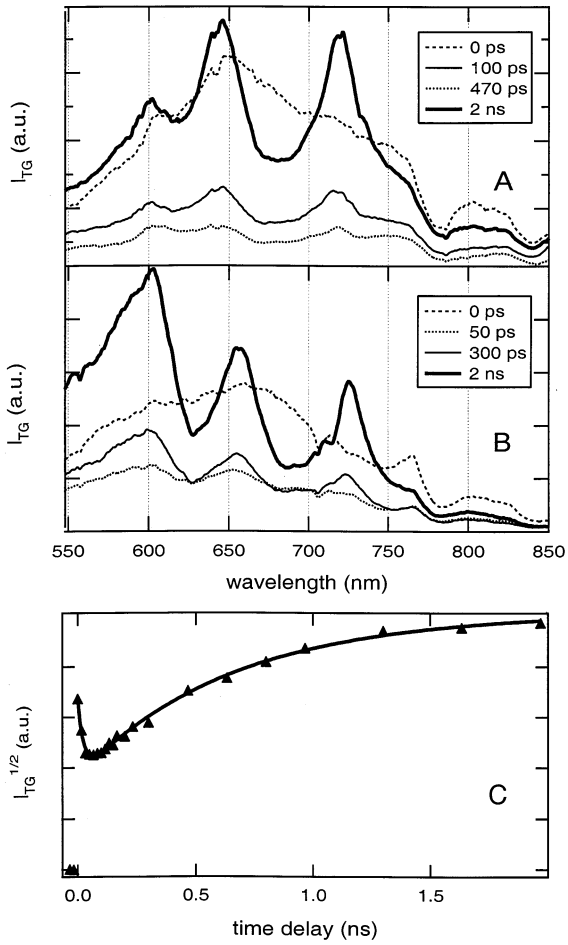

Figure 7. TG spectra measured at various time delays after excitation at 355 nm of solutions of (A) TrCA + 1 M IANI + 0.075 M DMA and (B) TeCA + 1 M IANI + 0.075 M DMA in ACN. (C) Time profile of the square root of the TG intensity at 600 nm measured with a solution TeCA + 1 M IANI + 0.075 M DMA in ACN. The continuous line is the best biexponential fit.

TABLE 1: Rate Constants and Quantum Yields Pertaining to the GIP Dynamics

A/D	k_{pop} (ns^{-1})	k_{SCR} (ns^{-1})	k_{TCR} (ns^{-1})	Φ_T	Φ_{ion} (with D_2)
DCA/ANI[30]	3.45	3.0		0	
DCA/BrANI	5.9	3.0[a]	2.45	0.41	0.13
DCA/IANI	42.05	1.6	40	0.95	0.27
TrCA/ANI[13]	15.8	15.2		0	
TrCA/IANI	≥ 105	≥ 13.5	≥ 91.5	0.87	0.87
TeCA/ANI[13]	47.6	47.6		0	
TeCA/IANI	≥ 143	≥ 26	≥117	0.82	0.82

[a] Assumed to be equal to k_{SCR}(DCA/ANI).

of the singlet precursor and sufficiently small to avoid a significant decrease of the polarity of the solution, which is a very important parameter in photoconductivity. The concentration of the secondary donor, DMA, was 5 mM. This ensures the full quenching of the relatively long-lived triplet state population and minimizes the quenching of the singlet precursor. However, the latter process could not be totally suppressed, and the amount of singlet quenching was determined by measuring the decrease of the steady-state fluorescence intensity of a solution of the acceptor with 0.1 M IANI upon addition of 5 mM DMA. The free ion yields corrected for this process are listed in Table 1. According to the above discussion, these ion yields can be considered as good estimates of the triplet yield for the corresponding system.

TABLE 2: Driving Forces for CS and CR with Various Cyanoanthracene/IANI Pairs

A	ΔG_{CS} (eV)[a]	ΔG_{SCR} (eV)	ΔG_{TCR} (eV)[b]
DCA	−0.15	−2.74	−1.08 to −0.93
TrCA	−0.43	−2.46	−0.80 to −0.65
TeCA	−0.61	−2.21	−0.55 to −0.40

[a] DCA: $E(S_1) = 2.88$ eV; $E_{red} = -0.98$ V vs SCE.[50] TrCA: $E(S_1) = 2.89$ eV; $E_{red} = -0.70$ V vs SCE.[48] TeCA: $E(S_1) = 2.82$ eV; $E_{red} = -0.45$ V vs SCE.[51] [b] With 1.66 eV[29] < $E(T_1)$ < 1.81 eV.[44]

The triplet yield obtained with TrCA and TeCA, as well as the upper limits for the ion population lifetime can now be used to determine both k_{TCR} and k_{SCR} (see Table 1).

Triplet quenching by a secondary donor was also investigated with DCA. With 1 M IANI and 5 mM DMA, the quenching of ^{3}DCA* and the ensuing $DCA^{\bullet-}$ formation could not be observed during the relatively small time window of the TG experiment. However, as shown in Table 1, photoconductivity measurements with 0.1 M IANI and 5 mM DMA indicate a substantial free ion yield. This yield is nevertheless about three times smaller than the triplet yield estimated above. The ion yield measured with 0.1 M BrANI and 5 mM DMA is also three times smaller than the triplet yield. This difference is most probably due to the weak driving force for the quenching of ^{3}DCA* by DMA. Indeed, depending on the triplet energy used for DCA, ($E(T_1) = 1.66-1.81$ eV),[29,44] the calculated driving force for ET with DMA amounts to -0.13 eV $\leq \Delta G_{CS} \leq +0.02$ eV. Therefore, this process should be slow compared with the lifetime of ^{3}DCA* in a liquid solution deoxygenated by simple argon bubbling and with the possible occurrence of external heavy atom effect due to the presence of 0.1 M BrANI or IANI.

Discussion

Influence of ΔG_{CS} on the Heavy Atom Effect. The results summarized in Table 1 indicate that the presence of a heavy atom on one of the reaction partners has a strong influence on the CR dynamics of the GIP. This effect is not new but has been until now only observed by monitoring the quenching product in a long time scale.[27-29,45-47] In this study, the formation of the triplet excited state upon geminate recombination is observed directly for the first time, and much more reliable rate constants can be deduced.

The mechanism responsible for this effect is most certainly SOC. In order for this mechanism to be operative, some orbital overlap in the GIP is required. In other words, SOC is only active in exciplexes (or CIPs). This indicates that the CR process investigated here occur while the ions are in close contact. This observation is rather surprising, because it is generally thought that exciplexes are only formed either upon direct excitation of a donor/acceptor complex or upon weakly exergonic ($\Delta G_{CS} \geq -0.4$ eV) diffusional ET quenching. More exergonic quenching ($\Delta G_{CS} < -0.4$ eV) should directly lead to the formation of so-called solvent separated or loose ion pairs (LIP).[48] For example, Gould et al. have reported that the exciplex formation efficiency upon diffusional ET quenching of cyanoanthracene derivatives by methyl-substituted benzenes decreases from 0.8 to 0.1 upon increasing the driving force from -0.37 to -0.65 eV.[49]

The situation observed here with anisole is clearly different, because the heavy atom effect on CR is observed even with a GIP formed upon quenching with $\Delta G_{CS} = -0.61$ eV (see Table 2). Therefore, CR occurs via an exciplex in all of the systems measured here. This exciplex is most certainly formed directly upon quenching and not after a collapse of a LIP. Indeed, the

TCR dynamics measured with TrCA and TeCA is so fast that essentially no conformational change can occur between CS and CR.

The formation of an exciplex upon quenching is not due to the large concentration of electron donor used for the ultrafast spectroscopy experiments. Indeed, the free ion yield measurements have been performed with only 0.1 M IANI, and the results are totally consistent with those performed at high concentration. Moreover, the formation of an exciplex is not due to the direct excitation of a ground state complex. First, no evidence of a ground state complex was found. Second, measurements performed upon 355 nm excitation are in total agreement with those carried out at 400 nm, and third, the excited singlet precursor is clearly observed by both TG and fluorescence up-conversion.

Therefore, it can be concluded that the quenching of cyanoanthracene derivatives by anisole results to an exciplex with essentially 100% efficiency at driving forces up to −0.61 eV.

In their investigation, Kikuchi and co-workers did not observe a heavy atom effect on both Φ_{sep} and Φ_T upon quenching of DCA by stronger electron donors, like iodoaniline (IANL) and iodoDMA (IDMA).[29] From this, they concluded that the primary product of quenching was a LIP and not an exciplex. Our data suggest that this conclusion might be too premature. Indeed, both Φ_{sep} and Φ_T are not the best parameters for evaluating the heavy atom effect on CR. It is not possible to determine k_{TCR}, which is the right measure of the heavy atom effect, from these two yields only. As $\Phi_{sep}/\Phi_T = k_{sep}/k_{TCR}$, k_{TCR} can only be calculated if k_{sep} is known, which was not the case in the investigation of Kukuchi and co-workers. Moreover, when the CR is ultrafast, the separation efficiency is close to zero and thus its precise determination is not possible. In this case, no reliable k_{TCR} value can be obtained, even if k_{sep} is known.

There is another possible explanation for the apparent absence of the heavy atom effect on CR with stronger electron donors. With those donors, SCR is no longer in the inverted region but rather in the barrierless regime and is thus ultrafast, as reported recently.[13] For example, the rate constants of CR to the ground state with DCA/DMA and DCA/ANL amount to 330 and 345 ns^{-1}, respectively.[13] If we assume similar k_{SCR} values with the halogenated donor, a substantial triplet yield requires k_{TCR} to be close to k_{SCR}. The driving force of TCR with IDMA and IANL is very small, between +0.03 and −0.12 eV for IDMA and between −0.02 and −0.17 eV for IANL, depending on the triplet energy used. Therefore, k_{TCR} cannot be expected to be as large as k_{SCR}. A triplet yield of 0.025 has been reported for the pair DCA/IANL.[29] This yield and $k_{SCR} \leq 345$ ns^{-1} result to $k_{TCR} \leq 9$ ns^{-1}. This value is smaller than those found with IANI, but this is in good agreement with a weak driving force. Therefore, the apparent absence of heavy atom effect can be very well accounted for by the relative magnitude of k_{SCR} and k_{TCR}.

Influence of ΔG_{TCR} on the Charge Recombination to the Triplet State. Figure 8 shows a plot of the free energy dependence of k_{TCR}. For comparison, the free energy dependence of k_{SCR} measured with various methoxy-substituted benzenes and cyanoanthracene derivatives and published in ref 13 is also reported. The continuous line is the best fit of the semiclassical expression of nonadiabatic electron transfer theory[15,52] to the k_{SCR} data. From this fit, the reorganization energy associated with solvent and other low-frequency modes, λ_s, amounts to 0.90 eV, the reorganization energy due to high-frequency modes, λ_v, is 0.41 eV (assuming an average frequency of 1500 cm^{-1}), and the electronic coupling matrix element V is 88 cm^{-1}. For

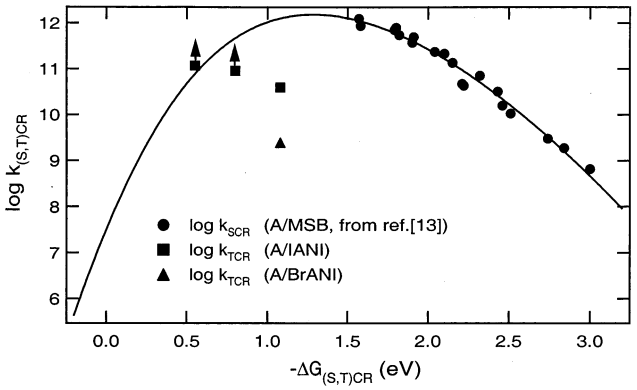

Figure 8. Free energy dependence of the TCR rate constants measured with A/IANI and A/BrANI and comparison with that measured for the SCR with cyanoanthracene derivatives and methoxy-substituted benzenes (MSB) (from ref 13).

k_{TCR}, one could expect in principle similar values of λ_s and λ_v, but a substantially smaller coupling constant V, because this process is not totally spin-allowed, despite the large SOC. In other words, the bell-shape curve for the free energy dependence of k_{TCR} should be similar to that found for k_{SCR}, but only shifted down.

From Figure 8, it is immediately clear that the free energy dependence of k_{TCR} cannot be reproduced by just shifting down the bell-shape curve found for k_{SCR}. With $\lambda_s = 0.9$ eV, TCR with TrCA and TeCA should be in the normal regime and, thus, slower than with DCA, contrarily to the observation. The only way to find some agreement between theory and the k_{TCR} values is to assume a much smaller reorganization energy, i.e., $\lambda_s \approx 0.3$ eV. Such a small λ_s is however difficult to justify.

In our recent investigation of the CR dynamics of a GIP formed upon ET quenching of a Zn-porphyrin in the S_2 state, we found rate constants of the order of 2.5 ps^{-1} for CR to the singlet excited state with a driving force smaller than −0.8 eV.[33] These large rate constants were explained by the effect of nonequilibrium dynamics. This competition between the relaxation of the GIP population to the equilibrium and its decay by CR has been recently shown to be a plausible explanation for the absence of normal region in CR of excited donor−acceptor complexes.[53]

For TrCA/IANI and TeCA/IANI, only lower limit values of k_{TCR} are known. An upper limit can be estimated by assuming that k_{SCR} with IANI is smaller or equal to k_{SCR} with ANI. Indeed, a GIP with a heavy atom is no longer in a pure singlet or triplet state, and thus, the electronic coupling matrix element V for SCR can be expected to be somewhat smaller than that for SCR in singlet GIP without a heavy atom. With this assumption and knowing the triplet yield, the upper limit of k_{TCR} with TrCA/IANI and TeCA/IANI is 100 and 220 ns^{-1}, respectively. The relaxation of the GIP after its formation involves mainly intramolecular and solvent modes. Essentially two processes occur during vibrational relaxation: (1) intramolecular vibrational redistribution (IVR), where the vibrational energy concentrated in the few ET active modes is redistributed among other modes, and (2) vibrational cooling (VC), where the temperature of the vibrationally hot molecule equilibrates with that of the bath. For large molecules in liquids, IVR occurs in a few tens to a few hundreds of fs, whereas VC takes place in a 10 ps time scale.[54−56] Therefore, TCR might occurs while the GIP is still vibrationally hot. Such "hot" CR has recently been reported for a GIP formed upon highly exergonic ET quenching.[13] The temperature of a GIP like $TeCA^{\bullet-}/IANI^{\bullet+}$

formed upon ET quenching with $\Delta G_{CS} = -0.61$ eV can be estimated to be around 380 K. Assuming a total reorganization energy of 1.3 eV, the TCR rate constant at 380 K can be estimated to be about 3 times as large as at 300 K. This increase is too small to account for the unusually fast TCR measured with this pair.

In ACN, relaxation of the solvent modes is ultrafast: inertial solvent motion occurs in a 50−100 fs time scale,[57−59] whereas a time constant of 500 fs has been reported for diffusive motion.[60] Therefore, CR must occur while the GIP is close to equilibrium.

Nevertheless one should not forget that the validity of the nonadiabatic ET theory is limited to charge transfer processes in weakly coupled systems.[15] The occurrence of a heavy atom effect indicates that the GIPs considered here are in fact exciplexes, where charge transfer is not complete. Therefore, the discrepancy between the prediction of this theory and the measured rate constants may just be due to the fact that the intermediates investigated here are too strongly coupled to be described with this model.

Concluding Remarks

The present investigation is a further confirmation that the presence of a neutral excited state located below the GIP state leads to a an acceleration of the CR, i.e., to a suppression of the inverted region. This effect has been also reported for CR of GIPs formed upon ET quenching of molecules in the S_2 state.[33,61,62] These observations support the hypothesis of the formation of an electronic excited product invoked to explain the absence of the inverted region in bimolecular ET quenching experiments.[63] However, the formation of excited ions in such reactions still remains to be proven.

This study also shows that the TCR of GIPs with a heavy atom is a very efficient way of populating the triplet state of a molecule with an intrinsically small triplet yield. We have shown here that a triplet yield close to unity can be achieved with a time constant of less than 10 ps. Such a fast triplet state population cannot be obtained by the more conventional triplet sensitization,[64] first because triplet−triplet energy transfer is generally slower than ET,[19] and second because this would require an impractically large concentration of energy acceptor.

This resulting triplet state population can react with a second, stronger, electron donor to produce free ions with a high quantum yield, as shown in Figure 7. Although apparently complex, this "zigzag" scheme is very efficient, because the first three charge transfer steps are moderately exergonic and thus intrinsically ultrafast and because the last unwanted CR to the neutral ground state is spin forbidden.

Finally, the occurrence of a substantial heavy atom effect with TeCA/IANI indicates that the −0.4 eV upper limit, often invoked for exciplex formation in polar solvents,[49,65] might be, in some cases at least, underestimated. Further investigation on the heavy atom effect with GIPs formed in more exergonic quenching processes are in progress.

Acknowledgment. This work was supported by the Fonds National Suisse de la Recherche Scientifique through project No. 2000-0632528.00.

List of Acronyms

CIP: contact ion pair
CS: charge separation
CR: charge recombination
ET: electron transfer
GIP: geminate ion pair
IVR: intramolecular vibrational redistribution
LIP: loose ion pair
SCR: singlet charge recombination
SOC: spin−orbit coupling
SSIP: solvent-separated ion pair
TCR: triplet charge recombination
TG: transient grating
VC: vibrational cooling

References and Notes

(1) A list of acronyms can be found at the end of the paper.
(2) Werner, H. J.; Schulten, Z.; Schulten, K. *J. Chem. Phys.* **1977**, *67*, 646.
(3) Mataga, N.; Asahi, T.; Kanda, Y.; Okada, T.; Kakitani, T. *Chem. Phys.* **1988**, *127*, 249.
(4) Masnovi, J. M.; Kochi, J. K. *J. Am. Chem. Soc.* **1985**, *107*, 7880.
(5) Peters, K. S.; Lee, J. *J. Phys. Chem.* **1992**, *96*, 8941.
(6) Song, L.; Swallen, S. F.; Dorfman, R. C.; Weidemaier, K.; Fayer, M. D. *J. Phys. Chem.* **1993**, *97*, 1374.
(7) Gould, I. R.; Farid, S. *Acc. Chem. Res.* **1996**, *29*, 522.
(8) Clark, C. D.; Hoffman, M. Z. *J. Phys. Chem.* **1996**, *100*, 7526.
(9) Kircher, T.; Löhmannsröben, H.-G. *Phys. Chem. Chem. Phys.* **1999**, *1*, 3987.
(10) Mataga, N.; Miyasaka, H. *Adv. Chem. Phys.* **1999**, *107*, 431.
(11) Vauthey, E. *J. Phys. Chem.* **2000**, *104*, 1804.
(12) Muller, P.-A.; Högemann, C.; Allonas, X.; Jacques, P.; Vauthey, E. *Chem. Phys. Lett.* **2000**, *326*, 321.
(13) Vauthey, E. *J. Phys. Chem. A* **2001**, *105*, 340.
(14) Neufeld, A. A.; Burshtein, A. I.; Angulo, G.; Grampp, G. *J. Chem. Phys.* **2002**, *116*, 2472.
(15) Marcus, R. A.; Sutin, N. *Biochim. Biophys. Acta* **1985**, *811*, 265.
(16) Kuznetsov, A. M.; Ulstrup, J. *Electron Transfer in Chemistry and Biology*; J. Wiley: Chichester, U.K., 1999.
(17) Haselbach, E.; Vauthey, E.; Suppan, P. *Tetrahedron* **1988**, *44*, 7335.
(18) Vauthey, E.; Henseler, A. *J. Photochem. Photobiol. A* **1998**, *112*, 103.
(19) Högemann, C.; Vauthey, E. *J. Phys. Chem. A* **1998**, *102*, 10051.
(20) Weller, A. *Z. Phys. Chem. N.F.* **1982**, *130*, 129.
(21) Steiner, U. E.; Haas, W. *J. Phys. Chem.* **1991**, *95*, 1880.
(22) Werner, H. J.; Staerk, H.; Weller, A. *J. Chem. Phys.* **1978**, *68*, 2419.
(23) Schulten, K.; Weller, A. *Biophys. J.* **1978**, *24*, 295.
(24) Roest, M. R.; Oliver, A. M.; Paddon-Row, M. N.; Verhoeven, J. W. *J. Phys. Chem. A* **1997**, *101*, 4867.
(25) Schulten, K.; Staerk, H.; Weller, A.; Werner, H. J.; Nickel, B. *Z. Phys. Chem. N.F.* **1976**, *101*, 371.
(26) Okada, T.; Karaki, I.; Matsuzawa, E.; Mataga, N.; Sakata, Y.; Misumi, S. *J. Phys. Chem.* **1981**, *85*, 3957.
(27) Steiner, U.; Winter, G. *Chem. Phys. Lett.* **1978**, *55*, 364.
(28) Föll, R. E.; Kramer, H. E. A.; Steiner, U. E. *J. Phys. Chem.* **1990**, *94*, 2476.
(29) Kikuchi, K.; Hoshi, M.; Niwa, T.; Takahashi, Y.; Miyashi, T. *J. Phys. Chem.* **1991**, *95*, 38.
(30) Vauthey, E.; Högemann, C.; Allonas, X. *J. Phys. Chem. A* **1998**, *102*, 7362.
(31) Goldschmidt, C. R.; Potashnik, R.; Ottolenghi, M. *J. Phys. Chem.* **1971**, *75*, 1025.
(32) Högemann, C.; Pauchard, M.; Vauthey, E. *Rev. Sci. Instrum.* **1996**, *67*, 3449.
(33) Morandeira, A.; Engeli, L.; Vauthey, E. *J. Phys. Chem. A* **2002**, *106*, 4833.
(34) Vauthey, E.; Pilloud, D.; Haselbach, E.; Suppan, P.; Jacques, P. *Chem. Phys. Lett.* **1993**, *215*, 264.
(35) von Raumer, M.; Suppan, P.; Jacques, P. *J. Photochem. Photobiol. A* **1997**, *105*, 21.
(36) Henseler, A.; Vauthey, E. *J. Photochem. Photobiol. A* **1995**, *91*, 7.
(37) Mattes, S. L.; Farid, S. *J. Am. Chem. Soc.* **1982**, *104*, 1454.
(38) Eichler, H. J.; Günter, P.; Pohl, D. W. *Laser-Induced Dynamic Gratings*; Springer-Verlag: Berlin, 1986.
(39) Fourkas, J. T.; Fayer, M. D. *Acc. Chem. Res.* **1992**, *25*, 227.
(40) Vauthey, E. *J. Phys. Chem. A* **1997**, *101*, 1635.
(41) Shida, T. *Electronic Absorption Spectra of Radical Ions*; Elsevier: Amsterdam, 1988; Vol. Physical Sciences data 34.
(42) Rice, S. A. In *Comprehensive Chemical Kinetics, Vol. 25, Diffusion-Limited Reactions*; Bamford, C. H., Tripper, C. F. H., Compton, R. G., Eds.; Elsevier: Amsterdam, 1985.
(43) Muller, P.-A. Facteurs influençant le transfert d'électron photoinduit. Ph.D. Thesis, University of Fribourg, 2001.

(44) Murov, S. L.; Carmichael, I.; Hug, G. L. *Handbook of Photochemistry*; Marcel Dekker: New York, 1993.
(45) Kikuchi, K.; Hoshi, M.; Abe, E.; Kokubun, H. *J. Photochem. Photobiol. A* **1988**, *45*, 1.
(46) Katsuki, A.; Akiyama, K.; Ikegami, Y.; Tero-Kubota, S. *J. Am. Chem. Soc.* **1994**, *116*, 12065.
(47) Shimada, E.; Nagano, M.; Iwahashi, M.; Mori, Y.; Sakaguchi, Y.; Hayashi, H. *J. Phys. Chem. A* **2001**, *105*, 2997.
(48) Kikuchi, K.; Takahashi, Y.; Hoshi, M.; Niwa, T.; Katagiri, T.; Miyashi, T. *J. Phys. Chem.* **1991**, *95*, 2378.
(49) Gould, I. R.; Young, R. H.; Mueller, L. J.; Farid, S. *J. Am. Chem. Soc.* **1994**, *116*, 8176.
(50) *Organic Photochemistry*; Mattes, S. L., Farid, S., Eds.; M. Dekker: New York, 1983; Vol. 6.
(51) Gould, I. R.; Moser, J. E.; Armitage, B.; Farid, S. *J. Am. Chem. Soc.* **1989**, *111*, 1917.
(52) Kestner, N. R.; Logan, J.; Jortner, J. *J. Phys. Chem.* **1974**, *78*, 2148.
(53) Nicolet, O.; Vauthey, E. *J. Phys. Chem. A* **2002**, *106*, 5553.
(54) Laermer, F.; Elsaesser, T.; Kaiser, W. *Chem. Phys. Lett.* **1989**, *156*, 381.
(55) Schwarzer, D.; Troe, J.; Zerezke, M. *J. Chem. Phys.* **1997**, *107*, 8380.
(56) Kovalenko, S. A.; Schanz, R.; Hennig, H.; Ernsting, N. P. *J. Chem. Phys.* **2001**, *115*, 3256.
(57) Rosenthal, S. J.; Xie, X.; Du, M.; Fleming, G. R. *J. Chem. Phys.* **1991**, *95*, 4715.
(58) Passino, S. A.; Nagasawa, Y.; Joo, T.; Fleming, G. R. *J. Phys. Chem.* **1997**, *101*, 725.
(59) Gumy, J. C.; Nicolet, O.; Vauthey, E. *J. Phys. Chem. A* **1999**, *103*, 10737.
(60) Horng, M. L.; Gardecki, J. A.; Papazyan, A.; Maroncelli, M. *J. Phys. Chem.* **1995**, *99*, 17311.
(61) Muller, P.-A.; Vauthey, E. *J. Phys. Chem. A* **2001**, *105*, 5994.
(62) Engeli, L.; Morandeira, A.; Muller, P.-A.; Vauthey, E. In *Femtochemistry and Femtobiology*; Douhal, A., Santamaria, J., Eds.; World Scientific: Singapore, 2002; p 314.
(63) Rehm, D.; Weller, A. *Isr. J. Chem.* **1970**, *8*, 259.
(64) Hviid, L.; Brouwer, A. M.; Paddon-Row: M. N.; Verhoeven, J. W. *ChemPhysChem* **2001**, *2*, 232.
(65) Kikuchi, K. *J. Photochem. Photobiol. A* **1992**, *65*, 149.